Derivation of electron-gas interatomic potentials from quantum-mechanical descriptions of ions in crystals

E. Francisco, J. M. Recio, M. A. Blanco, A. Martín Pendás, and L. Pueyo
Departamento de Química Física y Analítica, Facultad de Química,
Universidad de Oviedo, 33006 Oviedo, Spain
(Received 15 March 1994; revised manuscript received 1 June 1994)

The electron-gas-model theory is critically examined by means of interatomic potentials developed from *ab initio* quantum-mechanical descriptions of ions embedded in a crystalline environment and from the basic hypotheses of the model, namely, spherically symmetric and additive ionic electron densities, plus energy functionals for a homogeneous electron gas. We have found that the quantum-mechanical crystal potential enhances the deformation of the ionic wave functions induced by the crystal formation with respect to the self-consistent, crystal-adapted densities previously used in electron-gas simulations. Since these differences are dependent on the crystal strain, it is shown that some of the good results obtained in earlier electron-gas-based computations may be partially due to a cancellation effect between the assumptions of the model and the approximate description of the constitutive ions. For the test case explored here, the NaCl equation of state and the $B1$-$B2$ pressure-induced phase transition, the overall agreement with the experimental data is recovered when the electronic densities and the energetic interactions are both computed quantum mechanically.

I. INTRODUCTION

The most interesting chemical and physical behaviors of condensed matter are connected with its response to external agents such as pressure, temperature, and electromagnetic radiation. The knowledge and the understanding of the bulk, surface, and defective properties of materials under such conditions is therefore a matter where theoretical modeling needs to be developed in deep. The available *ab initio* quantum-mechanical methods that try to solve the Schrödinger equation of the solid are very effective on describing its static behavior, while the atomistic simulations based on interatomic potentials (IP's) constitute presently the only practical route to deal with the global characterization of the materials. Since the primary goal of theoretical modeling is prediction, it is clear that nonempirical derived IP's provide the natural choice to perform computer assisted simulations of solid materials at conditions that may not be attainable in the laboratory.

The information generated by the quantum-mechanical tools supposes both a severe test for the atomistic simulation and a valuable source for developing reliable IP's. Thus, much effort is currently dedicated to link accurate solutions of the Schrödinger equation to theoretical schemes that model the interatomic energy of molecules, clusters, and solids.[1–6]

One of the best known theoretical methods of atomistic simulation in ionic materials is the electron-gas (EG) theory of Gordon and Kim.[7,8] The three cornerstones on which the model rests are (i) the additivity of the ionic electron densities (IED's); (ii) the restriction of only spherically symmetric distortion allowed to the IED's; and (iii) the density functional algorithms used to compute the interaction energies. From 1972 up to date, the modifications in the EG model have been mainly addressed to the following two fronts: (i) the search for a greater accuracy of the density functionals from which the IP's are obtained, and (ii) the better descriptions of the IED's. In this work, our focus will lie in the analysis of the EG response to the quality of the IED's used in the calculations. Therefore, it is worthwhile to recall some of the previous reported contributions along this line.

Gordon and Kim[7] assumed that the IED's can be approximated by gas-phase Hartree-Fock IED's, which led to IP's that are pairwise additive and rigid. Improved versions of the initial Gordon and Kim EG model substituted the gas-phase IED's by IED's generated by including an approximated crystal potential in the ionic calculation. When the IED's are allowed to change under different crystal strains, a many-body contribution to the crystal energy appears through the so-called self-energy term, and the IP's move from rigid to relaxed. What has been invariably common to the generation of these relaxed IP's is the use of a Watson-type sphere[9] to mimic somehow the crystal potential. Muhlhausen and Gordon[10] chose the total charge of the sphere equal to minus the total ionic charge and the radius such that the potential at the anionic site coincides with the Coulombic crystal potential at that site. The same idea is also applied in the potential induced breathing model introduced by Boyer *et al.*,[11] in the EG approximation proposed by Mackrodt and Stewart,[12] and in the EG model of Hemley and Gordon.[13] Differences among these approaches appear in the description of the crystal potential and in the explicit calculation of the IED. Going further, Wolf and Bukowinski[14] selected the charge of the Watson sphere as Muhlhausen and Gordon did, but the radius in such a way as to minimize the total crystal energy. As a result of this additional requisite, the anionic

charge density suffers a greater contraction than in the previous Coulomb stabilized method of Muhlhausen and Gordon.[10] Wolf and Bukowinski pointed out that the neglect of this additional charge relaxation is probably one of the principal sources of error for the equations of state predicted by EG models.

In an effort to describe more accurately the IED's, Zhang and Bukowinski[15] proposed a modified local-density-type crystal potential containing Coulomb, exchange, and correlation contributions that is made self-consistent with the charge distribution of the ions in the crystal. In their calculations, the total potential is also simulated by a pseudo-Watson sphere.[15] The corresponding IP's derived from their IED's were able to provide a successful description of the equations of state (EOS's) and the pressure-induced transitions for several binary ionic halides and oxides and for the more covalent stishovite phase of SiO_2. In spite of the sophisticated iterative process followed to generate the IED's, Zhang and Bukowinski found that their potential yields anions that are only slightly smaller than those stabilized by a point-ion Coulomb potential.

As far as we know, no attempt has been made up to date to develop EG IP's using quantum-mechanical crystalline IED's that were self-consistent with the crystal potential they generate. A proper way to achieve such IED descriptions is to work out the canonical periodic Hartree-Fock equations of the compound. However, this method is not very appropriate to use in combination with EG models due to the intrinsic delocalized character of the (Bloch) orbitals resulting from the band-structure calculation. This inconvenience can be bypassed if the Hartree-Fock equations are iteratively solved within localized subspaces around every crystallographically different ion of the crystal. It might occur then that the IED's employed in some of the EG models commented above were very similar to those obtained from the quantum-mechanical self-consistent calculation in the compound of reference. Such a possibility would reinforce the plausibility of those EG models. However, this is a hypothesis that has not been yet tested and that deserves a detailed analysis due to the widespread use of the Gordon and Kim EG formulation.

It is our aim in this work to investigate the performance of the EG model when the IED's are obtained from the Hartree-Fock localized wave functions of the solid. We pursue rationalizing the potential answers of rigid and relaxed IP's in terms of the IED's used in their derivation and of the basic assumptions of the EG theory. This commitment involves the development of a new nonempirical procedure to generate EG crystal-consistent IP's that will be applied to the test case of the NaCl polymorphs. To obtain the quantum-mechanical descriptions of the ions embedded in the crystalline environment, we have used the *ab initio* perturbed ion (*ai*PI) model,[16,17] a variational quantum-mechanical method inspired on the theory of the electronic separability[18–20] that has been successfully applied to the description of a variety of electronic, structural, and thermodynamic properties of pure and defective crystals.[16,21–24] Within the *ai*PI framework, the electronic structure of every ion in the crystal is solved in a localized Fock space by breaking the crystal wave function into local group functions (atomic or ionic in nature). The minimization of the total crystal energy required by the Hartree-Fock approach provides a set of crystal-like atomic wave functions that respond self-consistently to the nearly exact crystal potential. This potential includes the Madelung contribution exactly evaluated by means of the Ewald transformation, a Coulombic correction due to the nonpunctual character of the ions,[25] a nonlocal exchange potential,[26,27] and a projection operator that tends to procure the atom-crystal orthogonality.[20] All the above terms of the crystal potential are explicitly incorporated in the Hamiltonian,[16] in contrast with the consideration of Watson parametrized spheres, as in the improved versions of the EG theory.[14] Besides, the IED solutions of the *ai*PI model satisfy both the self-consistent requisite with the crystal potential they generate and minimize the total energy of the crystal. Finally, it is really interesting to remark that the EG assumption of the total crystal density being a superposition of the individual IED's is better satisfied by the *ai*PI crystal-like orbitals than by the solutions employed in earlier EG calculations. This behavior is due to the appropriate representation of the quantum embedding effects, in particular of the Pauli repulsion incorporated in the *ai*PI crystal potential through the projection operator.[16] All these facts stress the relevance of analyzing the EG theory making use of IED's truly self-consistent with the crystal potential in which they are embedded.

The article is organized as follows. In Sec. II, we present the basic self-consistent Hartree-Fock *ai*PI equations and compare the IED's generated with this method with those obtained with approximate crystal potentials. Section III is dedicated to establish the computational parameters to be used in the EG model calculations and to generate the crystal-consistent IP's making use of the quantum-mechanical *ai*PI electron densities. Section IV is devoted to test the quality of the new derived IP's for a well-known test example: the NaCl crystal. Their response to structural, energetic, and thermodynamic properties is compared with previous EG model calculations, quantum-mechanical results, and experimental data. Finally, we summarize the more important conclusions of this work in Sec. V.

II. SELF-CONSISTENT CRYSTAL POTENTIAL AND IONIC ELECTRON DENSITIES

A. The Hartree-Fock *ai*PI equations

The self-consistent Hartree-Fock (HF) *ai*PI equation for the orbital ϕ_i of the ion A embedded in a crystalline environment is[16]

$$\left[H_i^0 + V_i^{\text{crystal}}\right]\phi_i = \varepsilon_i\phi_i, \tag{1}$$

where H_i^0 is the free-ion Hamiltonian and V_i^{crystal} is given by

$$V_i^{\text{crystal}} = \sum_{S(\neq A)} \left[V_{\text{eff}}^S(i) + P^S(i) \right], \tag{2}$$

S running over all the ions in the crystal except A. $V_{\text{eff}}^S(i)$ represents the crystal potential of the ith electron of A in the field due to the S ion:

$$V_{\text{eff}}^S(\mathbf{r}_{iS}) = -\frac{Z}{r_{iS}} + V_C^S(i) + V_X^S(i) = V_{\text{local}}^S(i) + V_X^S(i). \tag{3}$$

This effective potential contains nuclear attraction, Coulombic electronic repulsion, and exchange attraction contributions. We have decided to preserve the spherical symmetry of the ions in order to simplify the treatment. This approximation has been recently proved to yield accurate results within the EG framework for those ionic crystals in which the ions are not placed in very low symmetry positions.[6] The nuclear attraction plus the Coulombic repulsion due to a closed-shell ion S becomes then

$$V_{\text{local}}^S(r_1) = -\frac{Z}{r_1} + \int \rho^S(r_2) r_{12}^{-1} d\mathbf{r}_2 \ , \tag{4}$$

$\rho^S(r)$ being the IED of the ion S. $V_{\text{local}}^S(r)$ can be straightforwardly divided into a long-range classical term $V_{\text{class}}^S(r_1)$ plus a nonclassical electrostatic term $V_{\text{nc}}^S(r_1)$ that accounts for the diffuse character of the electronic cloud.

The nonlocal exchange operator V_X^S in Eq. (3) is conveniently approximated by its nondiagonal spectral resolution[26] over the basis functions centered at S. A detailed analysis of the errors introduced by this approximation has been presented by Martín Pendás *et al.* in Ref. 27.

$P^S(i)$ in Eq. (2) is a projector operator that enforces the orthogonality between the orbitals of the ion A and the orbitals of the ion S.[20] For a closed-shell ion this operator takes the form

$$P^S(i) = \sum_{g \in S} |\phi_g^S\rangle (-2\varepsilon_g^S) \langle \phi_g^S|, \tag{5}$$

where g runs over all occupied orbitals ϕ_g^S with orbital energies ε_g^S. This term has its origin in the HF version[19] of the theory of electronic separability[18] and plays a key role in the *ai*PI model. Its inclusion in V_i^{crystal} leads to solutions of Eq. (1) for different ions that are orthogonal in the limit of complete basis sets. This means that the hypothesis of describing the total crystal density as a superposition of the individual IED's, one of the essential approximations of the Gordon-Kim-type EG models, is really behind the *ai*PI formalism. However, as far as we know, a projector or any other operator enforcing orthogonality has not been included in the representation of the crystal potential of previous IED's generated for EG computations.

For our purposes, the relevant pieces of the output of the *ai*PI algorithm are the self-consistent IED's (ρ_A) for all the crystallographically nonequivalent ions of the crystal and their self-energies [$E_A(\rho_A)$]. Once the self-energies and the pairwise interactions have been obtained, the global properties of the solid are calculated as in other atomistic simulation techniques. Results generated with the above quantum-mechanical scheme, which is completely independent of any EG model approach, will be denoted in the following with the *ai*PI label.

B. Relaxation of the charge distributions

We analyze in this subsection the relative importance of the different contributions of V^{crystal} to the relaxation of the IED's. This relaxation is exclusively governed by the crystal potential once the geometrical configuration of the crystal and the basis sets for all the ions are specified. For this purpose, we have performed calculations using four different crystal models, labeled *class*, *Watson*, *local*, and *QM*. The *class* and *local* models use a crystal potential formed only by the point charge part (V_{class}) and the local part (V_{local}) of V^{crystal}, respectively. Model *QM* uses the total crystal potential V^{crystal} from the *ai*PI method. Finally, the *Watson* model is the crudest one and corresponds to approximate the crystal potential acting on the ion A by the Watson sphere:

$$V_{\text{Watson}} = \begin{cases} q^A/r & \text{for } r \geq \xi \ , \\ q^A/\xi & \text{for } r < \xi, \end{cases} \tag{6}$$

where q^A and ξ are the charge and the radius of the Watson sphere, chosen such that $V_{\text{Watson}} = V_{\text{class}}$ at the position of the ion A.

As test system, we have selected the NaCl crystal in the $B1$ phase. The IED's and the self-energies have been obtained using the high quality multi-ζ Slater-type orbitals of Clementi and Roetti[28] as input of the *ai*PI program.[17]

In Fig. 1, we plot the ionic radius (defined as the radius of the sphere that contains 99% of the electron density) of the *ai*PI solutions for Na^+ and Cl^- *versus* the lattice parameter **a**. The Na^+ ionic radius hardly suffers any change with **a** and is always essentially equal to the free-ion value, regardless the crystal potential used. On the contrary, the Cl^- ionic radius is highly dependent on the crystal potential. Thus, V_{class} produces a moderate contraction of its IED with respect to the free-ion value that increases with decreasing values of **a**. The use of the V_{Watson} representation for the V_{class} potential slightly emphasizes this contraction. V_{local}, exactly integrated in the *ai*PI model[17] except for the spherical average, turns to yield a pronounced expansion of the Cl^- IED. Finally, the *QM* crystal potential restores the expected contraction of the anionic electron density with respect to the free-ion value. Furthermore, this contraction is considerably more pronounced than the obtained with the two purely point charge potentials, V_{class} and V_{Watson}. It should be noticed that the above effects are enhanced as **a** decreases.

Since the EG pair interactions depend sensitively on the electronic charge in the overlap region, it is relevant to analyze the effect of the above crystal models on the rate

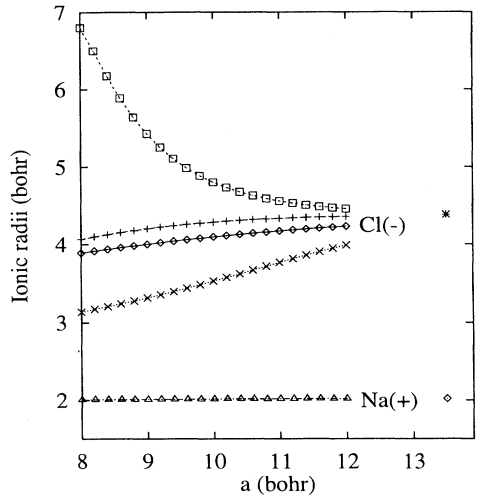

FIG. 1. Radii of the spheres containing 99% of the electron density of Na^+ and Cl^- versus the lattice parameter **a** in NaCl $B1$ phase. Results are shown corresponding to the use of several crystal potentials: *class* (+), *Watson* (◇), *local* (□), and *QM* (× and △). See text for the definition of these crystal potentials.

at which the Cl^- IED goes to zero. An appropriate way to visualize the differences in this rate among the four crystal potential models is to represent the logarithm of the electronic density *versus* the radial coordinate. The plot of the Cl^- IED at the theoretical *ai*PI equilibrium geometry of the NaCl $B1$ phase appears in Fig. 2. We observe again that, except in the inner region of the ion ($r < 2.5$ bohr), where all the crystal potentials yield a very similar answer, the *QM* model provides a more rapid decay of the electron density as we separate away from the nucleus than the other models. It is important to remark that the *class*, *Watson*, and *local* curves behave almost analogously to that one obtained with the free-ion solution. We believe that these results can be extended to other systems.

Support to this idea is found when we compare the *ai*PI solution for the O^{2-} ion in the MgO $B1$ phase (Fig. 1 of Ref. 21) with the corresponding IED obtained by Zhang and Bukowinski (Fig. 2 of Ref. 15). It is observed that the solution of Zhang and Bukowinski is very close to that obtained by Huzinaga and Hart-Davies for the O^{2-} free ion,[29] whereas the *ai*PI solution shows again a more contracted character.

The more pronounced shrinkage of the IED when the total crystal potential is used in the calculation has a quantum origin directly related with the projector $P^S(i)$. Due to the localized character of the *ai*PI method, an effective form of minimizing interionic overlaps is by means of a contraction of the IED's. This fact can be viewed as an additional attribute of the *ai*PI formalism which helps improving the fulfillment of the basic hypothesis of the EG model theory.

The effect of the four crystal potential models on the IED's can be quantitatively measured by means of the deformation energy, $E^A_{\rm def}$. This magnitude, defined as the self-energy of A in the crystal minus the free-ion self-energy of A,

$$E^A_{\rm def}(\rho_A) = E^A(\rho_A) - E^A(\rho^0_A), \tag{7}$$

is plotted for the Cl^- ion in Fig. 3. $V_{\rm class}$ yields values of $E^{Cl^-}_{\rm def}$ that are very small and that slightly increase when **a** decreases. $V_{\rm Watson}$ emphasizes again the effect of

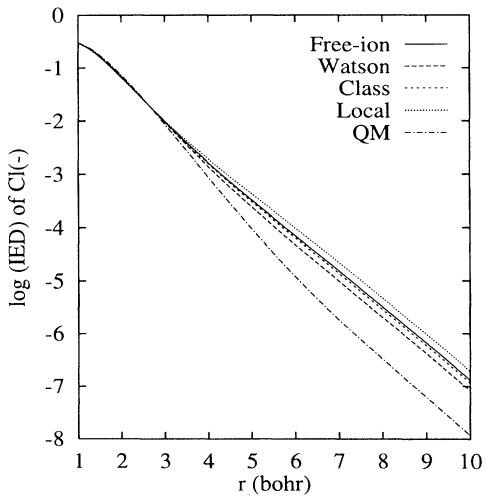

FIG. 2. Logarithm to base 10 of the ionic electron density (IED) of Cl^- versus the radial coordinate r according to several crystal potential models.

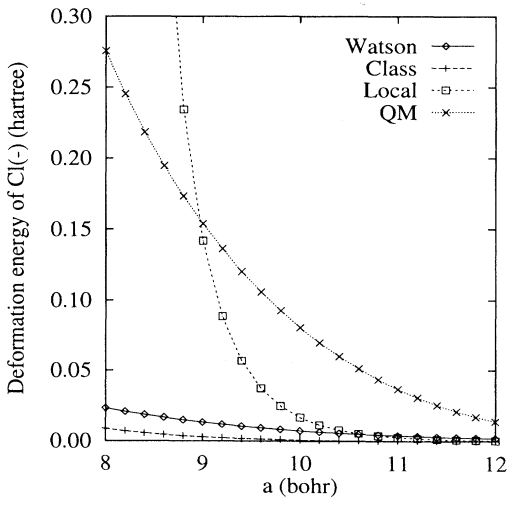

FIG. 3. Deformation energy of Cl^- versus the lattice parameter **a** according to several crystal potential models.

$V_{\rm class}$, whereas $V_{\rm local}$ gives values of $E_{\rm def}^{\rm Cl^-}$ that increase very sharply with decreasing **a**'s. Finally, the *QM* crystal potential produces values of $E_{\rm def}^{\rm Cl^-}$ much greater than the two point charge potentials, $V_{\rm class}$ and $V_{\rm Watson}$.

III. DEVELOPMENT OF CRYSTAL CONSISTENT INTERIONIC POTENTIALS

We develop in this section crystal-consistent EG model IP's using the IED's generated by the *ai*PI model. From now on, we will refer to these IP's as crystal-consistent IP's (CCIP's). In the first subsection, we detail the computational parameters used in the EG model calculations. In the second one, we parametrize the CCIP's in order to make the numerical explorations of Sec. IV easier.

A. Computational details

Once the IED's are available, the pairwise interaction energy between ions A and B, $V^{AB}(R;\rho)$, is computed in the EG theory as a sum of four contributions:

$$V^{AB}(R;\rho) = V^{E}(R;\rho) + V^{K}(R;\rho) + V^{X}(R;\rho) + V^{C}(R;\rho), \tag{8}$$

where R is the interionic separation, $\rho = \rho(\mathbf{a}) = \rho_A(\mathbf{a}) + \rho_B(\mathbf{a}) = \rho_A + \rho_B$, and $V^{E}(R;\rho)$, $V^{K}(R;\rho)$, $V^{X}(R;\rho)$, and $V^{C}(R;\rho)$ stand for Coulombic, kinetic, exchange, and correlation energy interactions, respectively. In terms of ρ_A, ρ_B, and ρ they are given by the following expressions:[7]

$$V^{E}(R;\rho) = \frac{Z_A Z_B}{R} + \int\int \frac{\rho_A(\mathbf{r}_1)\rho_B(\mathbf{r}_2)}{r_{12}} d\mathbf{r}_1 d\mathbf{r}_2 - Z_B \int \frac{\rho_A(\mathbf{r}_1)}{r_{1B}} d\mathbf{r}_1 - Z_A \int \frac{\rho_B(\mathbf{r}_2)}{r_{2A}} d\mathbf{r}_2 , \tag{9}$$

$$V^{I}(R;\rho) = \int d\mathbf{r} \left[\rho\epsilon^{I}(\rho) - \rho_A\epsilon^{I}(\rho_A) - \rho_B\epsilon^{I}(\rho_B)\right], \tag{10}$$

where ϵ^I ($I = K$, X, or C) are electron density functionals that can be chosen in several ways. In this work, we have used for ϵ^K, ϵ^C, and ϵ^X the functional forms of Thomas-Fermi,[7] Wigner (with the new fitting by Clementi),[30] and Handler,[31,32] given respectively by the expressions

$$\epsilon^{K}(\rho) = \frac{3}{10}(3\pi^2)^{\frac{2}{3}}\rho^{\frac{2}{3}}, \tag{11}$$

$$\epsilon^{C}(\rho) = -0.1890\rho^{1/3}\left[5.8032 + \rho^{1/3}\right]^{-1}, \tag{12}$$

and

$$\epsilon^{X}(\rho;N) = \frac{-5.744\ 49\rho^{2/3}}{\left[1 + a\rho^{p} + b\rho^{q} + c\rho^{r} + d\rho^{s}\right]^{Q}}, \tag{13}$$

where

$$a = 117.155\,10N^{-0.468\ 02},$$
$$b = 25.559\,99N^{-0.372\ 67},$$
$$c = 42.119\,50N^{0.184\ 59},$$
$$d = \left[\frac{11.488\ 98}{0.162\ 748N^{1.279\ 35}}\right]^{1.5s},$$

$p = 0.481\,00N^{0.101\,37}$, $q = 0.232\,73N^{-0.024\,536}$, $r = 0.443\,30N^{0.026\,373}$, $s = 1.072N^{0.031}$, $Q = 2/(3s)$, and $N = (N_A + N_B)/2$, N_A and N_B being the number of electrons of atoms A and B, respectively.

Numerical integrations of the density functionals involved in the EG models introduce some errors in the calculation. These errors, in principle, can be diminished by increasing the order of the quadrature. However, if an analytical integration is possible, this should always be preferred with respect to any numerical one. For this reason, the expression of $V^{E}(R;\rho)$ in Eq. (9) has been exactly evaluated in this article by means of powerful analytical algorithms recently developed.[25] This has been motivated by the observation that a careful numerical integration of the electron density of a given ion-ion pair did not give exactly a total number of electrons equal to the sum of the electrons of both ions.

To compute the integrals that appear in Eq. (10), we have used a spheroidal coordinate system.[7] The angular integration over ϕ is trivially 2π, since the electron density is cylindrically symmetric along the internuclear axis. In the cases of $\lambda = (r_A + r_B)/R$ and $\mu = (r_A - r_B)/R$, we have used a 60×60 Gauss-Legendre quadrature. The limits of λ and μ are $1 \le \lambda < \infty$ and $-1 \le \mu \le 1$. Since the Gauss-Legendre quadrature requires finite lower and upper limits,[33] the integration of λ must be carried out with some care. To solve this problem we have proceeded as follows. First, we compute the radii of the spheres containing 99.9998% of the IED's ($r_A^{\max}$ and $r_B^{\max}$). Second, we choose the upper limit of λ to be $\lambda^{\max} = 1 + \frac{2}{R}\max(r_A^{\max}, r_B^{\max})$. With this selection, the total volume of integration contains at least 99.9998% of the electron density.

B. Parametrization of interionic potentials and deformation energies

We have computed the Na^+-Cl^- and Cl^--Cl^- short-range pairwise energies in the NaCl $B1$ phase with **a** ranging from 8.0 to 12.0 bohrs at intervals of 0.2 bohr using the EG model computational parameters reported in the previous subsection. Some of these functions have been plotted in Fig. 4, where the short-range energies computed with free-ion electron densities are also shown for comparison. We have found that for any value of **a** greater than 8.0 bohrs the Na^+-Na^+ short-range energies are negligible. Therefore, these potentials will not be considered in the rest of the paper.

We observe from Fig. 4 that, at a given R, $V^{\rm NaCl}(R;\mathbf{a})$ and $V^{\rm ClCl}(R;\mathbf{a})$ increase their values with increasing

values of **a**, being the interactions $V^{\mathrm{NaCl}}(R;\infty)$ and $V^{\mathrm{ClCl}}(R;\infty)$ the more repulsive ones. Due to this fact, Gordon-Kim-type models using a single-crystalline IED for each ion must give values of $\mathbf{a}_e$ and E_{coh} smaller than those obtained with free-ion solutions. Note that this is the result predicted when using rigid IP's.

It is useful in practical calculations to represent the computed interatomic energies with analytical expressions. The regular changes shown by $V^{\mathrm{NaCl}}(R;\mathbf{a})$ and $V^{\mathrm{ClCl}}(R;\mathbf{a})$ with **a** and R allow us to establish the following three-step fitting procedure.

(i) Fit the $\{A_k,\alpha_k\}$ parameters of the following linear combination of exponentials

$$V^{AB}(R;\mathbf{a}) = \sum_k A_k(\mathbf{a}) R^{n_k} e^{-\alpha_k R}, \tag{14}$$

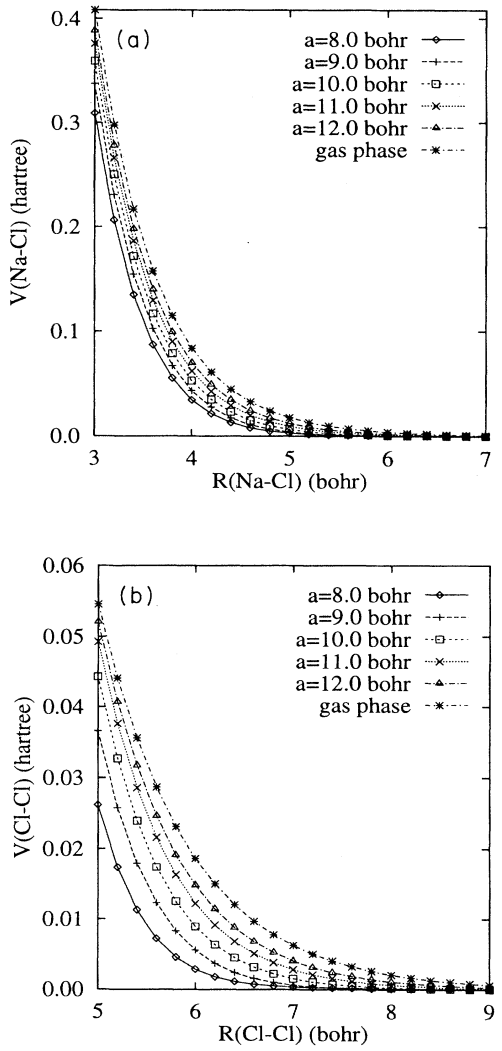

FIG. 4. Pairwise short-range interionic energies for the Na^+-Cl^- (a) and Cl^--Cl^- (b) pairs at different lattices parameters **a** according to our calculations.

to the computed $V^{\mathrm{NaCl}}(R;\mathbf{a}_e)$ and $V^{\mathrm{ClCl}}(R;\mathbf{a}_e)$ short-range energies, $\mathbf{a}_e$ being the *ai*PI theoretical equilibrium lattice parameter (10.58 bohrs for the NaCl $B1$ phase).

(ii) Repeat step (i) for all the lattice parameters at which the short-range energies were computed with the restriction of keeping the α_k parameters frozen at the values obtained in step (i) optimizing only the linear coeficients.

(iii) Fit a polynomial to the $A_k(\mathbf{a})$ values obtained in the previous step.

The final analytical forms for the Na^+-Cl^- and Cl^--Cl^- short-range pairwise CCIP's are collected in Table I. Along with these pairwise interionic energies, a term containing the deformation energy of the ions as a function of the lattice parameter changes must be taken into account to confer the appropriate relaxed attribute to the IP's. These terms can be approximately represented, in atomic units, by

$$E_{\mathrm{def}}^{\mathrm{Na}^+(B1)}(\mathbf{a}) = 2307.812\ 33 e^{-1.774\ 624\ 76\mathbf{a}} - 721.738\ 041\mathbf{a}^{-6}, \tag{15}$$

$$E_{\mathrm{def}}^{\mathrm{Cl}^-(B1)}(\mathbf{a}) = 249.499\ 405 e^{-0.746\ 459\ 27\mathbf{a}} - 123\ 574.800\mathbf{a}^{-6}. \tag{16}$$

We have included in these functions the differential correlation energy (crystalline minus free-ion) computed by means of the Clementi and Chakravorty method.[34] The relative importance of $E_{\mathrm{def}}^{\mathrm{Na}^+}$ and $E_{\mathrm{def}}^{\mathrm{Cl}^-}$ can be judged from the following values: At $\mathbf{a}$=10.60 bohrs $E_{\mathrm{def}}^{\mathrm{Na}^+(\mathrm{B1})} = -0.3$ Kcal/mol and $E_{\mathrm{def}}^{\mathrm{Cl}^-(\mathrm{B1})} = 2.6$ Kcal/mol. The corresponding values at $\mathbf{a}$=8.0 bohr are -0.8 Kcal/mol and 104.5 Kcal/mol. Thus, the deformation energy of Cl^- is far larger than that of Na^+, as corresponds to the more polarizable nature of the anion, in complete agreement with our discussion of the previous section (see Fig. 1). Besides, these numbers clearly show that not only the deformation energy of the ions at a given **a**, but also its variation with the crystal geometry, should be taken into account to analyze crystal properties.

IV. QUALITY TEST OF THE INTERIONIC POTENTIALS

The purpose of this section is to test the quality of the derived CCIP's. To this end, we compute the equilibrium lattice parameter ($\mathbf{a}_e$), the cohesive energy [$E_{\mathrm{coh}}(\mathbf{a}_e)$], the EOS and the $B1$-$B2$ pressure-induced transition data of the NaCl crystal. Although this system has been used as a test bed for quantum-mechanical methodologies,[16,35,36] only few calculations of the EOS and the phase stability have been reported for it. The exception is the extensive work of Löwdin[35] based on the HF approach. More recently, Froyen and Cohen[37] have investigated the structural behavior of NaCl under high pressure using a local-density approximation (LDA) pseudopotential method. Their results are in agreement with the room-temperature experimental data for NaCl. However, Feldman, Mehl, and Krakauer[38] have criticized

TABLE I. Short-range pairwise interionic potentials (Hartree) for the Na^+-Cl^- and Cl^--Cl^- pairs of NaCl in the $B1$ phase.

Na^+-Cl^-			
n_k	α_k	$A_k(\mathbf{a})=\sum_{j=1}^{2} C_{kj}\ \mathbf{a}^{j-1}$	$A_k(\infty)$
0	1.966 488 84	C_{11} =−1 796.494 02	1 026.413 66
		C_{12} =207.929 346	
-1	1.744 612 80	C_{21} =2 867.605 19	−1 355.663 50
		C_{22} =−3 10.333 389	

Cl^--Cl^-			
n_k	α_k	$A_k(\mathbf{a})=\sum_{j=1}^{4} C_{kj}\ \mathbf{a}^{j-1}$	$A_k(\infty)$
0	2.087 207 99	C_{11} =14 034.776 9	−4 892.426 23
		C_{12} =2 019.249 47	
		C_{13} =−751.194 907	
		C_{14} =37.489 758 3	
-1	1.699 803 30	C_{21} =−30 817.274 0	4 038.863 76
		C_{22} =4 102.443 57	
		C_{23} =83.062 470 6	
		C_{24} =−14.898 386 6	
-6	0.000 000 00	C_{31} =10 021.945 3	521.194 057
		C_{32} =−2 781.571 40	
		C_{33} =246.304 231	
		C_{34} =−6.884 470 19	

these results, and especially the good prediction of the transition pressure, and have concluded that extra energetic contributions beyond the LDA are needed to improve the agreement between theory and experiment. Regarding the results obtained from HF-type calculations, Recio *et al.*,[24] and Aprà *et al.*[39] have shown that the abscence of correlation energy effects introduces errors as large as 50% in the prediction of the zero P, T cohesive properties. A consistent global description of the NaCl crystal was only achieved after including correlation energy corrections in the case of the HF localized picture provided by the *ai*PI model.

In the first part of this section, we compare the CCIP results with theoretical values obtained by means of the above-cited quantum-mechanical methodologies and previous EG calculations, and with the available experimental data. In the second part, we analyze to what extent the CCIP's derived in the $B1$ phase are transferable to the $B2$ phase.

In our exploration, we use three types of CCIP's, labeled CCIP(ρ^0), CCIP(ρ^e), and CCIP(ρ). The CCIP(ρ^0)'s and CCIP(ρ^e)'s are rigid and use the free ion and the *ai*PI equilibrium geometry ($\mathbf{a}_e$=10.58 bohrs) solutions as frozen IED's, respectively. [The CCIP(ρ^0) set is a limit case of a crystal-consistent interatomic potential where the crystal embedding is removed.] Contrarily, the CCIP(ρ)'s are relaxed, as the IED's used in their derivation are the different *ai*PI solutions corresponding to different crystal geometries. The essential differences between the CCIP(ρ^0)'s and CCIP(ρ^e)'s for the Na^+-Cl^- and Cl^--Cl^- pairs are illustrated in Figs. 4(a) and 4(b). The corresponding curves for the CCIP(ρ)'s cannot be easily compared with those in the previous figures, since these potentials include many-body effects through the deformation energy contribution.

The comparison between the results obtained employing CCIP(ρ^0)'s and CCIP(ρ^e)'s gives us information on the effect introduced by pairwise rigid potentials with different repulsive characters over the crystal properties. The comparison between CCIP(ρ^0)'s or CCIP(ρ^e)'s and CCIP(ρ)'s will show us the importance of relaxing ρ in deriving the IP's. Finally, differences between the *ai*PI results and those obtained with the CCIP(ρ)'s are only due to the different expressions used to compute the pairwise interactions, as the many-body contributions are directly taken from the *ai*PI results. Their analysis allows the calibration of the energy density functionals used in EG model calculations.

A. Crystal properties of NaCl

Using the three types of CCIP's defined above, we have computed the cohesive energy of the NaCl $B1$ phase ($\mathbf{a}$ ranging from 8.0 to 12.0 bohrs) by means of a new computational code named PAIRPOT. Details of the program can be found elsewhere.[40,41] We have used in our computations an energy convergence threshold equal to 10^{-6} hartree. The properties explored here respond in a different manner to the type of calculation performed. Thus, as the short-range contribution to $E_{\rm coh}(\mathbf{a}_e)$ is around 11% of the total cohesive energy for NaCl, little influence on this magnitude is expected. However, as far as the $\mathbf{a}_e$ and the EOS are concerned, the dependence on the potentials is supposed to be larger, since the calculation of these properties involves derivatives of the $E_{\rm coh}(\mathbf{a})$ curve.

First of all, we would like to notice that the global

description of the zero T, P cohesive properties of NaCl provided by our CCIP computations is at least as successful as those given by other theoretical (quantum mechanical or EG) approaches (see Table II). It is also shown in Fig. 5 and Table II that, except for the CCIP(ρ^0) and the Aprà *et al.* calculations, the computed and the experimental values of $-E_{\rm coh}(\mathbf{a}_e)$ lie in the range 181–190 Kcal/mol. The low value obtained with the CCIP(ρ^0)'s (173.2 Kcal/mol) is due to the greater repulsive character of these potentials. This feature is also responsible for the larger $\mathbf{a}_e$ value predicted in the CCIP(ρ^0) calculation with respect to the CCIP(ρ^e) one. What is more interesting to remark from Fig. 5 is that the CCIP(ρ) EG calculation gives a stiffer binding energy curve than the one computed with the *ai*PI scheme. This behavior leads to a larger $\mathbf{a}_e$ in the CCIP(ρ) calculation (11.06 bohrs) than in the *ai*PI one (10.58 bohrs) (see Table II).

From these results, we conclude that the pairwise repulsive interaction computed with the energy density functionals is overestimated with respect to the quantum-mechanical result provided by the *ai*PI method. In Secs. II and III, we remarked that the many-body contribution to these potentials was underestimated with respect to the *ai*PI value, since the IED's used in their derivation do not differ so much from the gas-phase IED's as the local HF solutions do. Besides, it is necessary to stress that with the IED's and the pairwise interactions obtained following the Hartree-Fock localized scheme implemented in the *ai*PI model, the computed $\mathbf{a}_e$ is in good agreement with the experimental value (10.66 bohrs).

Considering these facts, the predictions obtained in other EG model calculations using relaxed IP's may now be foreseen: the overestimated repulsive pairwise interaction can be compensated by an underestimation of the many-body energy. The final balance may produce $\mathbf{a}_e$ values shorter than those obtained in our CCIP(ρ) calculation and thus in better agreement with the experiments (see Table II).

A similar analysis can be extended now to the discussion of the NaCl EOS. If we allow the IED's to readjust themselves at each different lattice parameter, as in the CCIP(ρ)-type calculations, we expect to find a more compressible crystal than with rigid CCIP(ρ^0) and CCIP(ρ^e) descriptions. The EOS is mainly determined by the bulk modulus (B_0) and its first pressure derivative (B_0'). Their values are collected in the last two columns of Table II. Although the CCIP(ρ^0) value for B_0 (23.3 GPa) is lower than the CCIP(ρ) one (26.2 GPa), the resulting $B(P)$ function (in the linear approximation) is clearly stiffer when using the rigid potentials. The predicted CCIP(ρ^e) value for B_0 is already higher than the one obtained with the relaxed potentials.

TABLE II. Static properties of NaCl ($B1$ phase) at zero temperature and pressure obtained in several calculations.

	$\mathbf{a}_e$ (bohr)	$-E_{\rm coh}$ (Kcal/mol)	B_0 (GPa)	B_0'
CCIP(ρ^0)	11.33	173.2	23.3	5.61
CCIP(ρ^e)	10.72	186.1	30.5	5.56
CCIP(ρ)	11.06	185.5	26.2	4.55
Ref. 35	10.39	183.2	21.7	-
Ref. 37	10.43	-	31.2	-
Ref. 38	10.45	-	28.7	5.0
Ref. 39	10.96	178.0	22.8	-
*ai*PI	10.58	189.6	28.9	4.75
Ref. 10	10.83	181.4	-	-
Ref. 13	10.65	184.0	29.0	-
Ref. 15	10.53	183.8	28.1	-
Expt.	10.66[a]	185.3[a]	28.5[b]	4.88[b]

[a]Extrapolated to 0 K by Brewer, quoted by Kittel, Ref. 48.
[b]Reference 45.

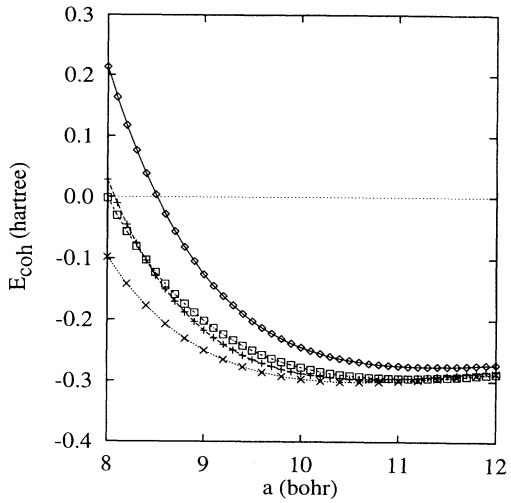

FIG. 5. Cohesive energy of NaCl in the $B1$ phase versus the lattice parameter **a**. The symbols ◇, +, and □ stand for the CCIP(ρ^0), CCIP(ρ^e), and CCIP(ρ) calculations, respectively. The symbol × represents the quantum-mechanical results obtained with the *ai*PI model.

The global result is also illustrated in Fig. 6, where the static normalized volume (V/V_0) versus P diagrams, generated from our $E_{\rm coh}(\mathbf{a})$ versus **a** curves, are plotted. We also include in this figure the room-temperature (RT) experimental data of Refs. 42, 43, and 44, and the extrapolated 0 K V/V_0-P curve that was obtained from higher T data[45] using a Vinet EOS fitting.[46] It is apparent here that the CCIP(ρ) curve represents the behavior of the softest crystal, which turns to be the experimentally RT observed conduct of NaCl. This result is fortuitous since our computations are performed for a static lattice (zero T, zero-point contributions neglected). It should be noticed that the *ai*PI predictions describe accurately the athermal corrected V/V_0-P curve. The collected values for B_0 (see Table II) from earlier EG computations agree again with thoses obtained quantum mechanically.

After the exploration of the $B1$ phase of NaCl, we discuss the data generated for the $B2$ phase and for the $B1$-$B2$ pressure-induced transition. The most interesting results are gathered in Table III. In this case, the CCIP (ρ^e)'s have been developed using the IED's obtained at the *ai*PI equilibrium geometry of the $B2$ phase (6.492 bohrs). For the CCIP(ρ)'s, we have used the IED's obtained at lattice parameters of the $B2$ phase ranging from 4.6 to 6.9 bohrs. This interval corresponds to a variation

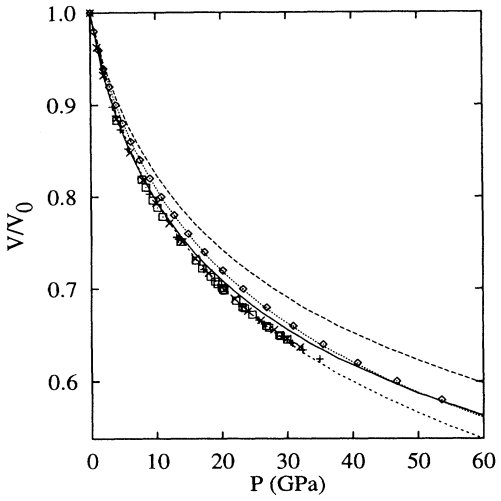

FIG. 6. Static V/V_0-P diagrams of NaCl in the $B1$ phase according to CCIP(ρ^0) (solid), CCIP(ρ^e) (long-dashed), CCIP(ρ) (short-dashed), and *ai*PI (dotted) calculations. The symbols □, ×, and + stand for the room-temperature data of Refs. 42, 43, and 44, respectively. Diamonds (◇) represent the 0 K extrapolated Vinet EOS.

of the nearest Na^+-Cl^- distance similar to that one used in the $B1$ phase. The first point to remark is that the relative order of the values obtained for $\mathbf{a}_e$ and $-E_{\rm coh}(\mathbf{a}_e)$ in the three CCIP models explored, in the *ai*PI scheme, and in earlier EG model calculations is identical to the one obtained in the $B1$ phase. Our previous argumentation is then reinforced. The same consistency has been found for the EOS and the B_0 and B_0' elastic parameters (for briefness only B_0 values are reported), with the exception of the surprising high value obtained for B_0 (37.31 GPa) by Zhang and Bukowinski.[15] Since this is the only number that breaks the observed trends among the different models used to analyze $\mathbf{a}_e$, $E_{\rm coh}(\mathbf{a}_e)$, and B_0, we suggest taking it with caution.

As regards the transition data, the expected predictions of the three CCIP EG computations and the comparison with the quantum-mechanical results and previous EG model calculations are difficult to guess due to the cancellation of effects between the two phases. This consideration should be born in mind when analyzing the results of Table III. A specific example illustrates this. The $B1$-$B2$ transition pressure, P_t, may be estimated as the quotient[47]

$$P_t = -\frac{E_{\rm coh}(B2) - E_{\rm coh}(B1)}{V_0(B2) - V_0(B1)} = -\frac{\Delta E_{\rm coh}}{\Delta V_0} \qquad (17)$$

where the energies and volumes are calculated at the corresponding equilibrium geometries at zero pressure.

We observe in Table III that the computed value for $\Delta E_{\rm coh}$ is very similar in the three CCIP calculations, in the Aprà *et al.* study,[39] and in the *ai*PI model. However, the $V_0(B2)/V_0(B1)$ quotient is higher in the CCIP EG models and in Ref. 39 than in the *ai*PI calculation. According to Eq. (17), these results would lead to a lower value for P_t in the *ai*PI calculation. This is the tendency followed by the tabulated values, that were obtained solving $G(B2)$=$G(B1)$, G being the static Gibbs free energy. We conclude again that the overestimated pairwise interaction, as computed with the energy density functionals, is the major responsibility for the anomalous computed high values of P_t [45.3 GPa in the CCIP(ρ) calculation]. Previous EG calculations using relaxed potentials predict lower values for P_t, which we explain as due in part to the balance introduced by the underestimation of the many-body deformation energy contribution to the cohesive energy.

TABLE III. Static properties of NaCl ($B2$ phase) at zero temperature obtained in several calculations.

	$\mathbf{a}_e$ (bohr)	$-E_{\rm coh}$ (Kcal/mol)	B_0 (GPa)	$V_0(B2)/V_0(B1)$	P_t (GPa)	$-\Delta V_t/V_t(B1)$
CCIP(ρ^0)	7.024	162.0 (11.2)[a]	22.8	0.952	29.0	0.071
CCIP(ρ^e)	6.609	175.9 (10.2)	32.1	0.937	34.6	0.058
CCIP(ρ)	6.852	175.1 (10.4)	27.1	0.951	45.3	0.047
CCIP(ρ)($B1$)	6.801	175.0 (10.5)	28.5	0.929	35.5	0.048
*ai*PI	6.492	178.8 (11.0)	25.6	0.923	22.0	0.113
Ref. 35	-	-	-	-	10.1	-
Ref. 37	-	-	-	-	27	0.058
Ref. 38	-	-	-	-	21.4	0.047
Ref. 39	6.746	168.7 (9.3)	24.4	0.933	39.2	0.043
Ref. 10	6.650	173.4 (8.0)	-	0.928	-	-
Ref. 13	6.546	176.8 (8.0)	-	0.929	18.5	0.070
Ref. 15	6.463	176.9 (6.9)	37.31	0.925	29	0.040
Expt.	-	-	36.2[b]	0.929[b]	26.8[c]-30[d]	0.058[d]

[a]The numbers in parentheses are $\Delta E_{\rm coh}$($B1$-$B2$).
[b]Room-temperature extrapolated to zero-pressure value of Heinz and Jeanloz, Ref. 49.
[c]Reference 50.
[d]Reference 51.

B. Transferability of the interionic potentials

A relevant matter in the development of crystal consistent IP's is to analyze if they are transferable between different phases of a crystal or from one crystal to another. It may be argued that the IP's generated with such a crystal specific procedure, as the one outlined in Sec. III, would not be able to describe the same interactions in other systems. However, we have seen that a reliable transference of the CCIP(ρ)'s potentials from the $B1$ to the $B2$ phase is possible, as long as both structures have the same reduced lattice spacing ($\mathbf{a}/\mathbf{a}_e$).

Since the relaxed CCIP(ρ)'s are determined by the $\rho(\mathbf{a})$ functions, it is clear that they will be transferable provided there exist a relationship between $\mathbf{a}(B1)$ and $\mathbf{a}(B2)$ satisfying $\rho^{B1}(\mathbf{a}^*) = \rho^{B2}(\mathbf{a}^*)$. We have found that such a relationship does exist by choosing $a^* = \mathbf{a}(B1)/\mathbf{a}_e(B1) = \mathbf{a}(B2)/\mathbf{a}_e(B2)$. This drives us to the conclusion that $\rho^{B1}(1) = \rho^{B2}(1)$, that is, ions in both phases show an essentially common IED at the corresponding equilibrium geometries.

In Fig. 7, the validity of the proposed transference scheme for the CCIP(ρ)'s is clearly illustrated. The pairwise Na^+-Cl^- and Cl^--Cl^- energies for the $B1$ and $B2$ phases at their corresponding zero-pressure equilibrium geometries are plotted in Figs. 7(a) and 7(b). From these two figures we observe that the curves of the $B1$ and $B2$ phases practically coincide. Similar plots for other lattice parameters provide pairs of alike curves as in this case. In Fig. 7(c), we plot the deformation energy of NaCl in the $B2$ phase versus the nearest Na^+-Cl^- distance (R_n) obtained from the IED's of the $B2$ phase and from the IED's of the $B1$ phase at equivalent reduced lattice parameters. The coincidence of both curves is again nearly perfect.

We conclude that the pairwise and many-body contributions to the CCIP(ρ)'s are transferable between the two crystalline phases, as long as the crystal geometries are identical when scaled with respect to the zero-pressure equilibrium values.

Our results for the equilibrium properties of the $B2$ phase obtained using the CCIP's generated from $B1$ IED's (see Table III) confirm the conclusion of the previous paragraph: $\mathbf{a}_e$, $E_{\rm coh}(\mathbf{a}_e)$, and B_0 values differ from those obtained with CCIP's generated from $B2$ IED's in less than 0.052 bohr, 0.1 Kcal/mol, and 1.5 GPa, respectively. For the phase transition properties the agreement is not so good, since these properties depend on differences between magnitudes computed in two different phases, and are therefore very sensitive to the details of the calculations.

To end with the analysis of the $B1$-$B2$ transferability, it is very important to mention that in our calculations, the quotient $\mathbf{a}_e(B1;P)/\mathbf{a}_e(B2;P)$ hardly changes with P. For instance, in the range of pressures going from 0 to 60 GPa, this quotient, as computed using the CCIP(ρ)'s generated from $B1$ IED's, is found to be 1.619 ± 0.015. Consequently, we arrive at a worthwhile conclusion: the quality of the transferability scheme proposed here is independent of pressure. This result also illustrates that

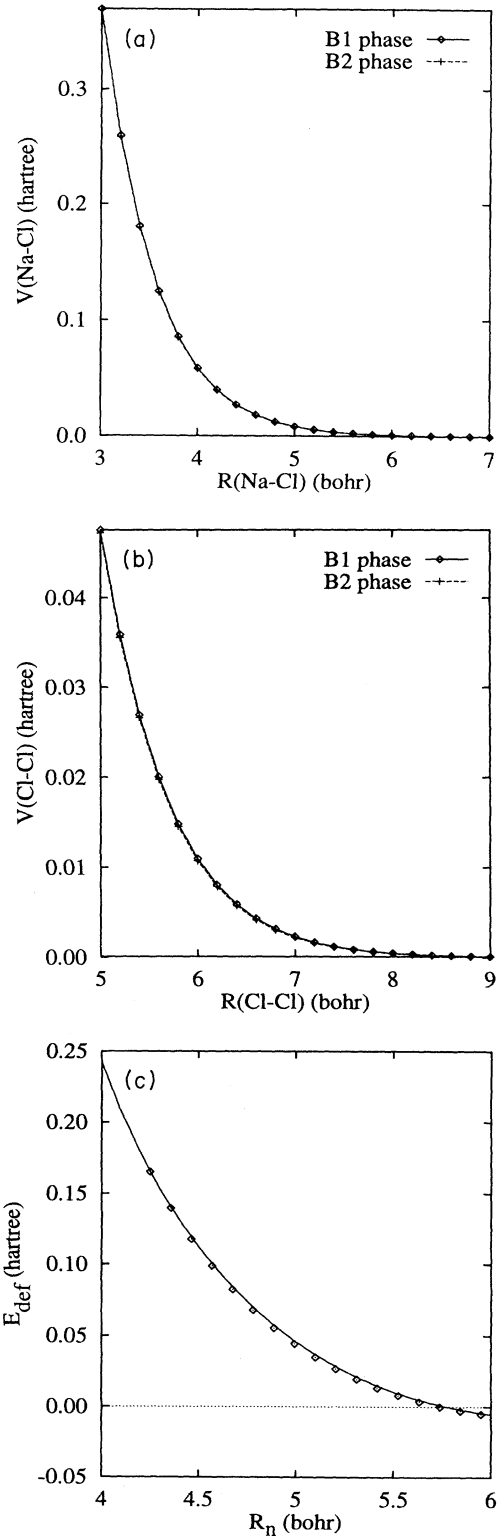

FIG. 7. Calculated short-range pairwise energies for the (a) Na^+-Cl^- and (b) Cl^--Cl^- pairs in the $B1$ ($\mathbf{a}$=10.58 bohrs) and the $B2$ ($\mathbf{a}$=6.492 bohrs) phases. (c) Deformation energy of NaCl in the $B2$ phase versus the nearest-neighbor distance (R_n). Symbols in (c) represent the values obtained from the IED's of the $B1$ phase using the transference scheme described in the text.

at any pressure the $B1$ and $B2$ phases of NaCl are well described with common, pressure-dependent, IED's.

V. CONCLUSIONS

Drawn by the increasing demand of reliable IP's to be used in computer simulations, we have critically examined in this paper one of the best known atomistic techniques in ionic materials: the Gordon and Kim EG model. Our contribution has mainly been dedicated to the study of the dependence of the EG-type IP's on the IED's employed in their generation. This task has been performed in two steps: (i) analysis of the IED response to a hierarchy of crystal models, and (ii) development of the so-called crystal-consistent IP's (CCIP's) and subsequent application of them to a test case: the NaCl crystal.

We have demonstrated that only a precise description of the quantum contributions to the crystal potential can account for the global contraction of the anionic IED and the increase of its self-energy upon crystal formation. The change of these two properties with the lattice parameter **a** is captured only to a small fraction of its total value with a classical lattice. It has also been shown that the *ai*PI IED's are better suited to fulfill the electron density additivity assumption of the EG theory than other IED's obtained with approximated crystal potentials.

A decisive test of the EG energy density functionals is performed when comparing a variety of cohesive and elastic properties obtained with the relaxed CCIP(ρ)'s and with the *ai*PI scheme. Our analysis shows that there exists an overestimation of the pairwise repulsive energy as calculated with the density functionals. A cancellation effect may appear if we combine these pairwise interactions with self-energies computed from approximate crystal-adapted IED's. This is a plausible explanation to some of the results previously obtained within the EG-model approach. We believe that this critical attitude opens new courses to investigate the basic hypotheses of the Gordon and Kim EG model.

ACKNOWLEDGMENTS

We are grateful to Professor V. Luaña and Professor M. Flórez for clarifying suggestions and careful reading of the manuscript and to the Centro de Cálculo Científico (Universidad de Oviedo) for the CONVEX facility in which the calculations have been done. One of us (M.A.B.) is also grateful to the Spanish Dirección General de Investigación Científica y Tecnológica (DGICYT) for a graduate grant. Financial support from the DGICYT, Project No. PB93-0327, is also acknowledged.

[1] E. Blaisten-Barojas and S. N. Khanna, Phys. Rev. Lett. **61**, 1477 (1988).
[2] R. Pandey and J. M. Vail, J. Phys.: Condens. Matter **1**, 2801 (1989).
[3] H. M. Lu and J. R. Hardy, Phys. Rev. Lett. **64**, 661 (1990).
[4] B. W. H. van Beest, G. J. Kramer, and R. A. van Santen, Phys. Rev. Lett. **64**, 1955 (1990).
[5] J. M. Recio, E. Francisco, M. Flórez, and A. Martín Pendás, J. Phys.: Condens. Matter **5**, 4975 (1993).
[6] D. J. Lacks and R. G. Gordon, Phys. Rev. B **48**, 2889 (1993), and references therein.
[7] R. G. Gordon and Y. S. Kim, J. Chem. Phys. **56**, 3122 (1972); Y. S. Kim and R. G. Gordon, Phys. Rev. B **9**, 3548 (1974); J. Chem. Phys. **60**, 4332 (1974).
[8] A. J. Cohen and R. G. Gordon, Phys. Rev. B **12**, 3228 (1975).
[9] R. E. Watson, Phys. Rev. **111**, 1108 (1958).
[10] C. Muhlhausen and R. G. Gordon, Phys. Rev. B **23**, 900 (1981); **24**, 2147 (1981).
[11] L. L. Boyer, M. J. Mehl, M. J. Feldman, J. R. Hardy, J. W. Flocken, and C. Y. Fong, Phys. Rev. Lett. **54**, 1940 (1985).
[12] W. C. Mackrodt and R. F. Stewart, J. Phys. C **12**, 431 (1979).
[13] R. J. Hemley and R. G. Gordon, J. Geophys. Res. **90**, 7803 (1985).
[14] G. A. Wolf and M. S. Bukowinski, Phys. Chem. Miner. **15**, 209 (1988).
[15] H. Zhang and M. S. T. Bukowinski, Phys. Rev. B **44**, 2495 (1991).
[16] V. Luaña and L. Pueyo, Phys. Rev. B **41**, 3800 (1990).
[17] V. Luaña, A. Martín Pendás, J. M. Recio, E. Francisco, and M. Bermejo, Comput. Phys. Commun. **77**, 107 (1993).
[18] R. McWeeny, Proc. R. Soc. London, Ser. A **253**, 242 (1959); *Methods of Molecular Quantum Mechanics* (Academic, London, 1989).
[19] S. Huzinaga and A. A. Cantu, J. Chem. Phys. **55**, 5543 (1971); S. Huzinaga, D. McWilliams, and A. A. Cantu, Adv. Quantum Chem. **7**, 187 (1973).
[20] E. Francisco, A. Martín Pendás, and W. H. Adams, J. Chem. Phys. **97**, 6504 (1992).
[21] V. Luaña, J. M. Recio, and L. Pueyo, Phys. Rev. B **42**, 1791 (1990).
[22] L. Pueyo, V. Luaña, M. Flórez, and E. Francisco, in *Structure, Interactions and Reactivity*, edited by S. Fraga (Elsevier, Amsterdam, 1992), Vol. B, pp. 504–526.
[23] V. Luaña and M. Flórez, J. Chem. Phys. **97**, 6544 (1992); V. Luaña, M. Flórez, and L. Pueyo, *ibid.* **99**, 7970 (1993); M. Flórez, M. A. Blanco, V. Luaña, and L. Pueyo, Phys. Rev. B **49**, 69 (1994).
[24] J. M. Recio, A. Martín Pendás, E. Francisco, M. Flórez, and V. Luaña, Phys. Rev. B **48**, 5891 (1993).
[25] A. Martín Pendás and E. Francisco, Phys. Rev. A **43**, 3384 (1991).
[26] S. Huzinaga, L. Seijo, Z. Barandiarán, and M. Klobukowski, J. Chem. Phys. **86**, 2132 (1987).
[27] A. Martín Pendás, E. Francisco, and J. M. Recio, J. Chem.

Phys. **97**, 452 (1992).
[28] E. Clementi and C. Roetti, At. Data Nucl. Data Tables **14**, 177 (1974).
[29] S. Huzinaga and A. Hart-Davies, Phys. Rev. A **8**, 1734 (1973).
[30] E. Clementi, S. J. Chakravorty, G. Corongiu, and V. Sonnad, in *Modern Techniques in Computational Chemistry: MOTECC-90*, edited by E. Clementi (ESCOM Science Publishers, Leiden, 1990), Chap. 2.
[31] G. S. Handler, J. Chem. Phys. **61**, 4824 (1974).
[32] G. Brual, Jr. and S. M. Rothstein, J. Chem. Phys. **69**, 1177 (1978); G. S. Handler (private communication).
[33] W. H. Press, B. P. Flannery, S. A. Teukolsky, and W. T. Vetterling, *Numerical Recipes* (Cambridge University Press, New York, 1986).
[34] S. J. Chakravorty and E. Clementi, Phys. Rev. A **39**, 2290 (1989).
[35] P. O. Löwdin, Adv. Phys. **5**, 1 (1956).
[36] A. B. Kunz, Phys. Rev. B **26**, 2056 (1982).
[37] S. Froyen and M. L. Cohen, J. Phys. C **19**, 2623 (1986).
[38] J. L. Feldman, M. J. Mehl, and H. Krakauer, Phys. Rev. B **35**, 6395 (1987).
[39] E. Aprà, M. Causà, M. Prencipe, R. Dovesi, and V. R. Saunders, J. Phys.: Condens. Matter **5**, 2969 (1993).
[40] Information regarding availability of PAIRPOT can be obtained by writing to A. M. Pendás (e-mail: *angel@hobbit.quimica.uniovi.es*).
[41] A. Martín Pendás, J. M. Recio, M. Flórez, V. Luaña, and M. Bermejo, Phys. Rev. B **49**, 5858 (1994).
[42] J. N. Fritz, S. P. Marsh, W. J. Carter, and R. G. McQueen, in *Accurate Characterization of the High Pressure Environment*, edited by E. C. Lloyd, Natl. Bur. Stand. (U.S.) Special Publications, Circ. No. 326 (U.S. GPO, Washington, DC, 1971), pp. 201–208.
[43] L. G. Liu, T. Takahashi, and W. A. Basset, J. Phys. Chem. Solids **31**, 1345 (1970).
[44] L. G. Liu and W. A. Basset, J. Appl. Phys. **44**, 1475 (1973).
[45] H. Spetzler, C. G. Sammis, and R. I. O'Connell, J. Phys. Chem. Solids **33**, 1727 (1972).
[46] P. Vinet, J. H. Rose, J. Ferrante, and J. R. Smith, J. Phys.: Condens. Matter **1**, 1941 (1989).
[47] J. A. Majewski and P. Vogl, Phys. Rev. Lett. **57**, 1366 (1986).
[48] C. Kittel, *Introduction to Solid State Physics* (Wiley, New York, 1971).
[49] D. L. Heinz and R. Jeanloz, Phys. Rev. B **30**, 6045 (1984).
[50] X. Li and R. Jeanloz, Phys. Rev. B **36**, 474 (1987).
[51] W. A. Basset, J. Takahashi, M. K. Mao, and J. S. Weaver, J. Appl. Phys. **39**, 319 (1968).